Periodica Polytechnica Mechanical Engineering, 63(3), pp. 165–170, 2019

The Wheeled Vehicle Forced Additional Turn Analytical Study

Vladimir Sistuk[1], Andrey Pikilnyak[2*]

[1] Department of Automobile Facilities, Transport Faculty, Kryvyi Rih National University, 44 Pushkin Street, 50002 Kryvyi Rih, Ukraine
[2] Department of Mechanical Engineering, Mechanical and Machine Engineering Faculty, Kryvyi Rih National University, 11 Vitaly Matusevich Street, 50027 Kryvyi Rih, Ukraine
[*] Corresponding author, e-mail: pikilnyak@gmail.com

Received: 02 June 2017, Accepted: 23 April 2019, Published online: 31 May 2019

Abstract

The study is dedicated to increasing open pit trucks with electrical transmission maneuverability indices. The possibility of forced controllability usage of rear traction wheels of open pit truck with the electrical transmission, which enables them to carry out maneuvers with the usage of a forced additional turn is presented. For the first time, there has been worked out a mathematical model of the forced additional turn. It enables to determine a correlation of rotational speed ratio of rear traction wheels of starboard and port sides of the wheeled vehicle relative to a tire-to-surface friction coefficient. Firstly, the analytical dependences, which allow predicting the indices of open pit trucks maneuverability while using the forced additional turn are determined. The mathematical model adopted to appropriate truck's electric drive control algorithm can lead to trucks performance increasing by means of maneuvering time reducing.

Keywords

wheeled vehicle, open pit truck, maneuverability, turning radius, forced additional turn

1 Introduction

The dominating mining method in Ukraine is open-pit one, which involves 92 % of the total iron ore mining, and the major industrial transport, which used for 90–95 % of mined rock hauling, are BelAZ open pit trucks with electrical transmission and payload capacity of 120–136 tones [1-8].

The overall trend of open-cut mining development in the region is rapid open pits deepening to 400 meters. This necessitates to load distances increasing and to further operating area parameters reduction. The operating site width is more than 25–35 meters, which is a lower limit for these trucks maneuvering under the design specifications. The transport facilities operating conditions deteriorating is so critical that load maneuver time already takes up to 26 % of the total haul cycle. Thus vehicles fuel consumption is increased and emergency events are occurred such as trucks sliding from the operating sites surfaces, dangling off their wheels and even roll-over.

While the depth of open pits has reached than their extension in the plan is tied to additional overburden operations for operating sites width increasing that can't be provided at this life stage of deposits, because there is a high probability of open-pit side buckling failure.

The analysis revealed that one way to pit trucks efficiency upgrading in open pits tight working space is the trucks maneuvering abilities improvement [9]. At AC electric traction drive the automatic control system allows to control the motor's rotation forcibly and individually for the rear wheel of starboard and port side if it's necessary to rim pulls difference increasing, which provides additional yaw moment also creating the so-called phenomenon of "additional forced turn" as the vehicle maneuver benefit.

2 Formulation of the problem

Until the present, this method of turn hasn't been widespread on vehicles principally because mathematical relationships for its characterization have been absent. In this regard, the additional forced turn mathematical model development is a priority.

The modelling includes the additional forced turn dynamics study (contact forces analysis, road resistance moment determination), the law of rotational speed ratio of rear traction wheels of starboard and port vehicle sides according to tire-to-surface friction coefficient. Finding of this law provides the appearance of the additional forced

Cite this article as: Sistuk, V., Pikilnyak, A. "The Wheeled Vehicle Forced Additional Turn Analytical Study", Periodica Polytechnica Mechanical Engineering, 63(3), pp. 165–170, 2019. https://doi.org/10.3311/PPme.11103

turn and pit truck maneuverability parameters definition which can be obtained in this ratio performance.

3 Materials and methods

The kinematic method of a vehicular spin is carried out via yaw moment, which is created by front directive wheels. The turning radius decreasing is possible by mean of the yaw moment increment. Whereas front wheel turning angles cannot be above the maximum design value, which is a function of wheelbase, front and rear wheel-tread and other features, the possibilities of the turning radius decreasing are limited by rotational speed ratio between rear traction wheels appropriate distantly and close-in to the turning point side. If the rotational speed ratio of the rear traction wheels of starboard and port sides of the vehicle are increased forcibly as consistent with some functional connection at the maximum value of front wheels turning angle, it creates the additional yaw moment, which leads to the shortening of turning radius. With the aim of a forced additional turn implementation besides of the rotational speed ratio of starboard and port side rear traction wheels changing it is necessary to ensure rim pulls distribution between the rear wheels according to a ground contacting area external resistance. The adjustment of rim pulls difference in compliance with tire-to-surface friction coefficient is required for a steady-state maneuver, because clear coordination will provide the demandable yaw moment for the forced additional turn, which is directed in opposition to a road resistance moment. This well-posed problem requires the function definition of the abovementioned physical magnitude.

The road resistance moment of the rear axle depends on cornering forces, N·m [10]

$$M_{rr} = b \cdot \left(R_{y3} - R_{y4}\right) \tag{1}$$

where R_{y3}, R_{y4} – are the general cornering forces of the rear axle wheels (N), b – is the distance of a center line of mass to the rear axle (m).

The general road resistance moment is governed by the general cornering forces of the corresponding axle wheels.

On the other hand, it is possible to specify the road resistance moment by dint of the approaches, which are used in tracked vehicles motion theory. These vehicles are maneuver at low speeds with huge movement resistance and create a significant caterpillar slippage toward to the ground contacting area. These features satisfy the conditions of a pit truckload maneuver.

Let's divide the elementary area in wheel mounting surface (Fig. 1) and assume that the turning point of directive tire imprint coincides with its geometric center. Based on the known approaches of the tracked vehicles motion theory [11], an elementary contact force, which is acting on the wheeled mover on the side of the ground contacting area can be represented as the following Eq. (2), (N):

$$dS = \varphi \cdot q \cdot dxdy \ , \tag{2}$$

where q – is the vehicle load on the wheel, (N), φ – is the tire-to-surface friction coefficient.

The tire-to-surface friction coefficient is determined by the difference of wheels rotational speeds in an accurate period of time

$$\varphi = \frac{(\omega_{ii} - \omega_{ei}) \cdot r_k \cdot 2 \cdot L}{g \cdot t \cdot a} \tag{3}$$

where ω_{ii}, ω_{ei} – are the initial and end rotational speeds of the wheels, rad/s; r_k – is the kinematic wheel radius, which is taken to be equal to dynamic one, m; a – is the coordinate of the vehicle mass center, m; L – is the wheelbase, m; t – is the time interval, s; g – is the acceleration of gravity, m/s^2.

Then, at any tire pressure distribution on-loading and flat spot form, the static road resistance moment for the individual wheel will be determined as follows, (N·m)

$$M_{rri} = \frac{\varphi}{b_1 \cdot l} \cdot S_i \int_0^{b_1}\int_0^{l} x \ dx \ dy \ , \tag{4}$$

where b_1 – is the width of the flat spot, l – is the length of the flat spot, (m).

Let's suppose that the dynamic road resistance moment is equal to the static one, which is taking place

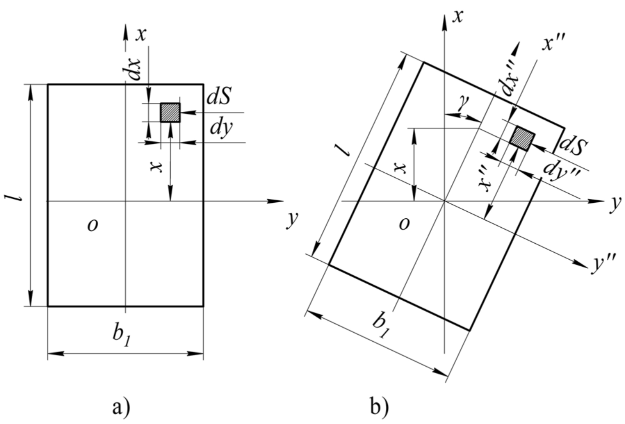

Fig. 1 The contact force that creates the road resistance moment: *a*) – for a non-turn drive wheel; *b*) – for a directive idle wheel

at motionless state for low maneuvering speeds. With considering the normal loads on the wheels, the front wheels turning angles, the size of flat spots, including rear axle twin wheels flat spots, and the tire-to-surface friction coefficient an equation of open pit truck road resistance moment will be as the following Eq. (5), (N·m):

$$M_r = \frac{\varphi \cdot m \cdot g \cdot b}{b_1 \cdot l \cdot 2 \cdot L}\int_0^{b_1}\int_0^{l}\frac{x}{\cos\gamma_1}dxdy + \frac{\varphi \cdot m \cdot g \cdot b}{b_1 \cdot l \cdot 2 \cdot L}\int_0^{b_1}\int_0^{l}\frac{x}{\cos\gamma_2}dxdy + \frac{\varphi \cdot m \cdot g \cdot a}{2 \cdot b_1 \cdot l \cdot 2 \cdot L}\int_0^{b_1}\int_0^{l} x\ dxdy + \frac{\varphi \cdot m \cdot g \cdot a}{2 \cdot b_1 \cdot l \cdot 2 \cdot L}\int_0^{b_1}\int_0^{l} x\ dxdy \tag{5}$$

where m – is the truck weight, (kg); b – is the coordinate of the vehicle mass center, (m); γ_1, γ_2 – are the directive wheels turning angles, (grad); x, y – are the coordinates of the elementary contact forces, (m).

If to eliminate the common factor Eq. (5) from the brackets, we will obtain

$$M_r = \frac{\varphi \cdot m \cdot g \cdot b}{2 \cdot b_1 \cdot l \cdot L}\int_0^{b_1}\int_0^{l} x\ dxdy \cdot \left(a + \frac{b}{\cos\gamma_1 + \cos\gamma_2}\right). \tag{6}$$

Thus, the road resistance moment is a friction torque, which occurs in the flat spot. It's uniquely determined by the friction area size, normal loads and friction coefficient. The above coefficient, which is the frictional rest estimation rate, is usually more than motion friction coefficient for the same surface [9].

It's well known, that steady-state turn existence condition is equality of the yaw moment, which is caused by rim pulls difference to the road resistance moment [10].

Thus, the steady-state turn existence condition can be presented in the following Eq. (7):

$$\sum_{i=1}^{n} M_{ti} = \sum_{i=1}^{n} M_{ri}\ , \tag{7}$$

where n – is the number of wheels.

The relationship between the difference of torques, which are generated by the transmission mechanisms, the ground contacting area characteristics (tire-to-surface friction coefficient) and wheel loads will be established to further forced additional turn dynamics study.

The traction wheel tangential force is a circumferential force which is generated by a torque and directed along wheels velocity vector, so the known equation (Eq. (8)) has the form [10, 12]:

$$R_{xi} = P_{wi} = P_{rpi} + P_{fi} + \frac{M_{jw}}{r_k} \tag{8}$$

where P_{fi} – is the rolling resistance force, N; P_{rpi} –is the rim pull, N; M_{jw} – is the wheel moment of inertia.

The yaw moment created by the difference of the circumferential forces is determined by that dependence, neglecting the wheel moment of inertia (stable motion with $d\omega_k / dt = 0$) and taking into account the rolling resistance:

$$M_t = \left(P_{w3} - P_{w4}\right)\cdot\frac{B_2}{2} = \left(\left(P_{rp3} + R_{z3}\cdot f\right) - \left(P_{rp4} + R_{z4}\cdot f\right)\right)\cdot\frac{B_2}{2} \tag{9}$$

where B_2 –is the rear wheel tread, m.

Let's assume that with high turning angles and low speeds the normal load between wheels of the opposite side of the respective axis is distributed equally, N:

$$R_{z3} = R_{z4} = \frac{m \cdot g \cdot a}{2 \cdot L}\ , \tag{10}$$

so

$$M_t = \left(R_{x3} - R_{x4}\right)\frac{B_2}{2} = \left(P_{rp3} - P_{rp4}\right)\frac{B_2}{2} = \left(\frac{T_3}{r_d} - \frac{T_4}{r_d}\right)\frac{B_2}{2}\ , \tag{11}$$

where R_{x3}, R_{x4} – is the tangential forces of the rear axle wheels, N; r_d – is the dynamic wheel radius, m.

Thus, at a turn, the circumferential forces which are created by a powertrain have the same value as the rim pulls and tangential forces with the same vehicle load distribution between the traction wheels that is present at low speeds.

4 Results and discussion

By equating Eq. (6) and Eq. (11), the relationship between rear traction wheels torques difference and the tire-to-surface friction coefficient was obtained, N·m:

$$\Delta T = T_4 - T_3 = \frac{\frac{\varphi \cdot m \cdot g}{b_1 \cdot l \cdot L}\int_0^{b_1}\int_0^{l} x \cdot dxdy \cdot \left(a + \frac{b}{\cos\gamma_1} + \frac{b}{\cos\gamma_2}\right)}{B_2}\ . \tag{12}$$

Thus, relies on Eqs. (6), (12), tire-to-surface friction coefficient increasing necessitates the yaw moment augmentation and, therefore, increasing of engine power consumption for the forced additional turn.

At the same time, if there is a loss of traction the rear wheel of the starboard side falls faster in slippage than the wheel of the port side. In this case, a further yaw moment increasing is possible by the port side rear wheel reversal of rotation.

The attitude equation of wheel motion brings us to the conclusion that there is a direct proportion between the torque and wheel rotational speed. This premise helps to exchange the rotational speed ratio of rear traction wheels by its torque ratio:

$$d\omega_i = \frac{T_i}{M_{jw}} dt \ , \tag{13}$$

where $d\omega_i$ – is the wheel rotational speed increment, rad/s.

Therefore, we have

$$\lambda = \frac{T_3}{T_4} \ , \quad \lambda = \frac{T_3}{T_3 - \Delta T} \ , \quad \lambda = \frac{T_4 + \Delta T}{T_4} \ , \tag{14}$$

where λ – is the rotational speed ratio of rear traction wheels.

Hence, considering Eq. (12), the law of the rotational speed ratio of rear traction wheels to the tire-to-surface friction coefficient and the torques of the wheels will be as follows:

$$\left.\begin{aligned} \lambda &= \frac{T_3}{T_3 - \dfrac{\left[\dfrac{\varphi \cdot m \cdot g}{b_1 \cdot l \cdot L}\displaystyle\int_0^{b_1}\int_0^{l} xdxdy \cdot \left(a + \dfrac{b}{\cos\gamma_1} + \dfrac{b}{\cos\gamma_2}\right)\right] \cdot r_d}{B_2}} \\ \lambda &= \frac{T_4 + \dfrac{\left[\dfrac{\varphi \cdot m \cdot g}{b_1 \cdot l \cdot L}\displaystyle\int_0^{b_1}\int_0^{l} xdxdy \cdot \left(a + \dfrac{b}{\cos\gamma_1} + \dfrac{b}{\cos\gamma_2}\right)\right] \cdot r_d}{B_2}}{T_4} \end{aligned}\right\} . \tag{15}$$

Considering Eqs. (14), (15), with acquainted rotational speed ratio of rear traction wheels the following torque dependencies must be fulfilled:

- for the rear wheel of the starboard side

$$T_3 = \frac{\left[\dfrac{\varphi \cdot m \cdot g}{b_1 \cdot l \cdot L}\displaystyle\int_0^{b_1}\int_0^{l} xdxdy \cdot \left(a + \dfrac{b}{\cos\gamma_1} + \dfrac{b}{\cos\gamma_2}\right)\right] \cdot r_d \cdot \lambda}{B_2 \cdot (\lambda - 1)}, \tag{16}$$

- for the rear wheel of the port side

$$T_4 = \frac{\left[\dfrac{\varphi \cdot m \cdot g}{b_1 \cdot l \cdot L}\displaystyle\int_0^{b_1}\int_0^{l} xdxdy \cdot \left(a + \dfrac{b}{\cos\gamma_1} + \dfrac{b}{\cos\gamma_2}\right)\right] \cdot r_d}{B_2 \cdot (\lambda - 1)} . \tag{17}$$

By solving together Eqs. (10)–(12), let's find rim pulls relationships to tire-to-surface friction coefficient at the forced additional turn, N:

$$P_{rp3} = \frac{T_4}{r_d} - R_{z3} f + R_{z4} f + \frac{\dfrac{\varphi \cdot m \cdot g}{b_1 \cdot l \cdot L}\displaystyle\int_0^{b_1}\int_0^{l} xdxdy \left(a + \dfrac{b}{\cos\gamma_1} + \dfrac{b}{\cos\gamma_2}\right)}{B_2} \tag{18}$$

$$P_{rp4} = \frac{T_3}{r_d} + R_{z3} f - R_{z4} f - \frac{\dfrac{\varphi \cdot m \cdot g}{b_1 \cdot l \cdot L}\displaystyle\int_0^{b_1}\int_0^{l} xdxdy \left(a + \dfrac{b}{\cos\gamma_1} + \dfrac{b}{\cos\gamma_2}\right)}{B_2} . \tag{19}$$

With allowance for Eq. (8), appropriate tangential forces formulas are depicted, N:

$$R_{x3} = \frac{T_4}{r_d} + \frac{\dfrac{\varphi \cdot m \cdot g}{b_1 \cdot l \cdot L}\displaystyle\int_0^{b_1}\int_0^{l} xdxdy \cdot \left(a + \dfrac{b}{\cos\gamma_1} + \dfrac{b}{\cos\gamma_2}\right)}{B_2} \tag{20}$$

$$R_{x4} = \frac{T_3}{r_d} - \frac{\dfrac{\varphi \cdot m \cdot g}{b_1 \cdot l \cdot L}\displaystyle\int_0^{b_1}\int_0^{l} xdxdy \cdot \left(a + \dfrac{b}{\cos\gamma_1} + \dfrac{b}{\cos\gamma_2}\right)}{B_2} . \tag{21}$$

So, for the forced additional turn it is necessary to provide some rim pulls of rear traction wheels of starboard and port sides via the powertrain, which are vary by dependences Eqs. (18), (19). Based on Eqs. (20), (21) can be argued that tangential forces of starboard and port side wheels differ from one another by a quantity of motion resistance force, N:

$$P_r = \frac{\dfrac{\varphi \cdot m \cdot g}{b_1 \cdot l \cdot L}\displaystyle\int_0^{b_1}\int_0^{l} xdxdy \cdot \left(a + \dfrac{b}{\cos\gamma_1} + \dfrac{b}{\cos\gamma_2}\right)}{B_2} . \tag{22}$$

With tire-to-surface friction coefficient increasing the torques that applied to the rear wheels should be enhanced in accordance with established dependences Eqs. (16), (17).

The motion resistance force Eq. (22) depends on the turning radius because the larger wheel moving causes the greater resistance to this displacement. In this regard, an important task is to determine the impact of the tire-to-surface friction coefficient on the vehicle turning radius.

For tracked vehicles with skid steering, this impact is presented in the form of overtaking caterpillars turning radius dependence on the so-called "resistance to motion factor", and in a turning resistance torque dependence on the turning radius of the machine [11]. However, for a heavy hauling and transport equipment, which are open-pit trucks, the turning radius dependence on the friction coefficient is not presented in open sources.

While taking the pull-transport equipment turning radius constant and independent from the friction is unacceptable hypothesis [12-15]. In this regard, another pit truck resistance to motion study is required to find this relationship.

Given the following expression

$$R_{x3} = \frac{T_4 \cdot \omega_4}{V_4} + \frac{\frac{\varphi \cdot m \cdot g}{b_1 \cdot l \cdot L} \int_0^{b_1} \int_0^{l} x dx dy \cdot \left(a + \frac{b}{\cos \gamma_1} + \frac{b}{\cos \gamma_2} \right)}{B_2} \tag{23}$$

$$R_{x4} = \frac{T_3 \cdot \omega_3}{V_3} - \frac{\frac{\varphi \cdot m \cdot g}{b_1 \cdot l \cdot L} \int_0^{b_1} \int_0^{l} x dx dy \cdot \left(a + \frac{b}{\cos \gamma_1} + \frac{b}{\cos \gamma_2} \right)}{B_2} \tag{24}$$

after mathematical transformations the rotational speed ratio of rear traction wheels can be represented by Eqs. (14), (23), (24):

$$\lambda = \frac{\frac{T_4}{r_d} + \frac{\frac{\varphi \cdot m \cdot g}{b_1 \cdot l \cdot L} \int_0^{b_1} \int_0^{l} x dx dy \cdot \left(a + \frac{b}{\cos \gamma_1} + \frac{b}{\cos \gamma_2} \right)}{B_2}}{\frac{T_3}{r_d} - \frac{\frac{\varphi \cdot m \cdot g}{b_1 \cdot l \cdot L} \int_0^{b_1} \int_0^{l} x dx dy \cdot \left(a + \frac{b}{\cos \gamma_1} + \frac{b}{\cos \gamma_2} \right)}{B_2}} . \tag{25}$$

Thus, for the first time, a law of the rotational speed ratio of rear traction wheels was obtained, which is necessary to provide in accordance to tire-to-surface friction coefficient while pit truck maneuvering by means of the forced additional turn Eq. (25).

Using Eq. (25), dependences of maneuverability kinematics parameters (turning radii) on tire-to-surface friction coefficient and rear wheels torques with the forced additional turn can be elucidated.

The pit truck turning radius is determined, m

$$R_{tr} = \frac{\frac{T_3}{r_d} \cdot B_2 + \frac{\varphi \cdot m \cdot g}{b_1 \cdot l \cdot L} \int_0^{b_1} \int_0^{l} x dx dy \cdot \left(a + \frac{b}{\cos \gamma_1} + \frac{b}{\cos \gamma_2} \right)}{\frac{T_4}{r_d} - \frac{T_3}{r_d} + 2 \cdot \frac{\frac{\varphi \cdot m \cdot g}{b_1 \cdot l \cdot L} \int_0^{b_1} \int_0^{l} x dx dy \cdot \left(a + \frac{b}{\cos \gamma_1} + \frac{b}{\cos \gamma_2} \right)}{B_2}} \cdot \frac{1}{\cos \gamma_1} . \tag{26}$$

Other maneuverability parameters can be defined by Eq. (25).

The distance from the turning point to the axis of port side rear wheels, m

$$R_1 = \frac{\frac{T_3}{r_d} \cdot B_2 - \frac{\varphi \cdot m \cdot g}{b_1 \cdot l \cdot L} \int_0^{b_1} \int_0^{l} x dx dy \cdot \left(a + \frac{b}{\cos \gamma_1} + \frac{b}{\cos \gamma_2} \right)}{\frac{T_4}{r_d} - \frac{T_3}{r_d} + 2 \cdot \frac{\frac{\varphi \cdot m \cdot g}{b_1 \cdot l \cdot L} \int_0^{b_1} \int_0^{l} x dx dy \cdot \left(a + \frac{b}{\cos \gamma_1} + \frac{b}{\cos \gamma_2} \right)}{B_2}} . \tag{27}$$

The distance from the turning point to the rear axle, m

$$R = \frac{\left[\frac{T_3}{r_d} + \frac{T_4}{r_d} \right] \cdot B_2}{2 \cdot \left[\frac{T_4}{r_d} - \frac{T_3}{r_d} + 2 \cdot \frac{\frac{\varphi \cdot m \cdot g}{b_1 \cdot l \cdot L} \int_0^{b_1} \int_0^{l} x dx dy \cdot \left(a + \frac{b}{\cos \gamma_1} + \frac{b}{\cos \gamma_2} \right)}{B_2} \right]} . \tag{28}$$

The distance from the turning point to the axis of starboard rear wheels, m

$$R_2 = \frac{\frac{T_4}{r_d} \cdot B_2 + \frac{\varphi \cdot m \cdot g}{b_1 \cdot l \cdot L} \int_0^{b_1} \int_0^{l} x dx dy \cdot \left(a + \frac{b}{\cos \gamma_1} + \frac{b}{\cos \gamma_2} \right)}{\frac{T_4}{r_d} - \frac{T_3}{r_d} + 2 \cdot \frac{\frac{\varphi \cdot m \cdot g}{b_1 \cdot l \cdot L} \int_0^{b_1} \int_0^{l} x dx dy \cdot \left(a + \frac{b}{\cos \gamma_1} + \frac{b}{\cos \gamma_2} \right)}{B_2}} . \tag{29}$$

Finally, a generic mathematical model of the forced additional turn is presented by a set of the equations:

$$\left. \begin{array}{c} A = \frac{\varphi \cdot m \cdot g}{b_1 \cdot l \cdot L} \int_0^{b_1} \int_0^{l} x dx dy \cdot \left(a + \frac{b}{\cos \gamma_1} + \frac{b}{\cos \gamma_2} \right) \\ R_{x3} = \frac{T_4 \cdot \omega_4}{V_4} + \frac{A}{B_2}; \quad R_{x4} = \frac{T_3 \cdot \omega_3}{V_3} - \frac{A}{B_2} \\ \lambda = \frac{T_4 / r_d + A / B_2}{T_3 / r_d - A / B_2} \\ R_{tr} = \frac{T_3 / r_d \cdot B_2 + A}{T_4 / r_d - T_3 / r_d + 2 \cdot A / B_2} \cdot \frac{1}{\cos \gamma_1} \end{array} \right\} . \tag{30}$$

5 Conclusion

For the first time mathematical model of the forced additional turn was developed which allows to determine a correlation of rotational speed ratio of rear traction wheels and to predict the wheeled vehicles kinematics parameters (indices of maneuverability) relative to the tire-to-surface friction coefficient and distribution of torques between the rear traction wheels on the basis of firstly determined analytical dependences. Thus, these dependences create the mathematical connection between kinematic and dynamic parameters of the wheeled vehicle forced additional turn.

References

[1] Vesnin, A. V., Sistuk, V. O., Bogachevskiy, A. O. "The analysis of mining conditions influence to operating time of dump trucks traction drive components", Metallurgical and Mining Industry, (3), pp. 268–271, 2015. [online] Available at: https://www.metaljournal.com.ua/assets/Journal/english-edition/MMI_2015_3/036%20(1)%20Vesnin.pdf [Accessed: 13 June 2017]

[2] Vesnin, A. V., Sistuk, V. O., Bogachevskiy, A. O. "The industrial dust properties as a wear factor of pit trucks electric machines elements", Metallurgical and Mining Industry, (3), pp. 272–275, 2015. [online] Available at: https://www.metaljournal.com.ua/assets/Journal/english-edition/MMI_2015_3/036%20(2)%20Vesnin.pdf [Accessed: 13 June 2017]

[3] Vesnin, A. V., Sistuk, V. O., Bogachevskiy, A. O. "Computer modeling usage for heat mass exchange inside mine dump-truck traction generator and electrical motor research", Metallurgical and Mining Industry, (3), pp. 276–278, 2015. [online] Available at: https://www.metaljournal.com.ua/assets/Journal/english-edition/MMI_2015_3/036-3-Vesnin.pdf [Accessed: 13 June 2017]

[4] Vesnin, A. V., Sistuk, V. O., Bogachevskiy, A. O. "Mathematical models analysis for the thermal state of mining trucks traction motors determining", Metallurgical and Mining Industry, (3), pp. 279–282, 2015. [online] Available at: https://www.metaljournal.com.ua/assets/Journal/english-edition/MMI_2015_3/036%20(4)%20Vesnin.pdf [Accessed: 13 June 2017]

[5] Morkun, V., Morkun, N., Pikilnyak, A. "Adaptive control system of ore beneficiation process based on Kaczmarz projection algorithm", Metallurgical and Mining Industry, (2), pp. 35–38, 2015. [online] Available at: https://www.metaljournal.com.ua/assets/Journal/english-edition/MMI_2015_2/007Morkun%20Pikilnyak.pdf [Accessed: 13 June 2017]

[6] Pikilnyak, A. "Adaptive control system of the iron ore flotation using a control action based on high-energy ultrasound", Metallurgical and Mining Industry, (2), pp. 27–30, 2015. [online] Available at: https://www.metaljournal.com.ua/assets/Journal/english-edition/MMI_2015_2/005Pikilnyak.pdf [Accessed: 13 June 2017]

[7] Pikilnyak, A. "The gas bubble size parameters monitoring and control method", Metallurgical and Mining Industry, (7), pp. 19–21, 2015. [online] Available at: https://www.metaljournal.com.ua/assets/Journal/english-edition/MMI_2015_7/004Andrey%20Pikilnyak%2019-21.pdf [Accessed: 13 June 2017]

[8] Frimpong, S., Galecki, G., Li, Y., Suglo, R. "Dump Truck Tire Stress Simulation for Extended Service Life", Transactions of the Society for Mining, Metallurgy, and Exploration, 332, pp. 422–429, 2012.

[9] Zhou, H., Wang, G., Ding, Y., Yang, J., Liang, C., Fu, J. "Effect of Friction Model and Tire Maneuvering on Tire-Pavement Contact Stress", Advances in Materials Science and Engineering, 2015, Article ID: 632647, 2015.
https://doi.org/10.1155/2015/632647

[10] Lindeque, G. C. "A critical investigation into tyre life on an iron ore haulage system", Journal of the Southern African Institute of Mining and Metallurgy, 116(4), pp. 317–322, 2016.
https://doi.org/10.17159/2411-9717/2016/v116n4a3

[11] Ahangaran, D. K., Yasrebi, A. B., Wetherelt, A., Foster, P. "Real–time dispatching modelling for trucks with different capacities in open pit mines", Archives of Mining Sciences, 57(1), pp. 39–52, 2012.
https://doi.org/10.2478/v10267-012-0003-8

[12] Volontsevich, D., Duong, S. H., Veretennikov, I. "Analysis of curvilinear motion of tracked vehicles with electromechanical dual-flux turning mechanisms", Eastern-European Journal of Enterprise Technologies, 3(7), pp. 21–28. 2016.
https://doi.org/10.15587/1729-4061.2016.71982

[13] Dabbs, H. D., Stemler, E. D., Cowper, L. M., Shults, R. F., Caterpillar Inc., "Differential steering control for a continuously variable transmission machine", USA, US 2008/0153662 A1, 2008.

[14] Yang, Y., Emadi, A. "Integrated electro-mechanical transmission systems in hybrid electric vehicles", In: Vehicle Power and Propulsion Conference, Chicago, IL, USA, 2011, pp. 1–6.
https://doi.org/10.1109/VPPC.2011.6042985

[15] Pacejka, H. B. "Tire and Vehicle Dynamics", 3rd ed., Butterworth-Heinemann, Oxford, UK, 2012.
https://doi.org/10.1016/B978-0-08-097016-5.01001-9